Bipolar spectroelectrochemistry.

David Ibañez,* Aranzazu Heras, and Alvaro Colina*

Department of Chemistry, Universidad de Burgos, Pza. Misael Bañuelos s/n, E-09001 Burgos, Spain.

ABSTRACT: Bipolar electrochemistry is receiving growing attention in the last years, not only because it is an important tool for studying electron transfer processes, but also because it is really fruitful in the development of new analytical sensors. Bipolar electrodes show promising applications as a direct analytical tool since oxidation and reduction reactions take place simultaneously on different parts of a single conductor. There are several electrochemical devices that provide information about electron transfer between two immiscible electrolyte solutions, but to the best of our knowledge, this is the first time that a bipolar device is able to record two spectroelectrochemical responses concomitantly at two different compartments. It allows deconvolving the electrochemical signal into two different optical signals related to the electron transfer processes occurring at two compartments that are electrically in contact. The combination of an electrochemical and two spectroscopic responses is indeed very useful, providing essential advantages in the study of a huge variety of systems. The study of three different electrochemical systems, such as reversible redox couples, carbon nanotubes and conducting polymers has allowed us to validate the new cell and to demonstrate the capabilities of this technique to obtain valuable time-resolved information related to the electron transfer processes.

Bipolar electrochemistry has traditionally been limited to industrial applications, such as metallurgy, chemical engineering and energy targets.[1–4] During the last decade, however, new devices have been developed and used in different fields,[5–10] making bipolar electrochemistry one of the most promising analytical tools in sensor applications.[11–13] The combination of bipolar electrochemistry and electrochemiluminescence is particularly interesting because it is an extremely sensitive detection method. In this way, the characterization of the electrochemiluminescence triggered by bipolar electrochemistry[14–18] has become the base for the development of new devices, providing spectroscopic and electrochemical information simultaneously. One of the most important points of interest in bipolar setups is the bipolar electrode, as it exhibits different electrochemical behaviors: on one side of the electrode surface an oxidation process takes place, while a reduction process is concomitantly observed on a different part of the same electrode. The simultaneous analysis at separate locations of the bipolar electrode can be performed using different setup configurations. On one hand, in the open configuration the bipolar electrode is located inside of a unique electrolyte solution. On the other hand, in the closed configuration, the electrolyte solution is separated in different compartments, one for the anodic reaction and the other one for the cathodic process.[16,19]

Electrochemistry at the interface between two immiscible electrolyte solutions (ITIES) has become one of the most interesting systems in electrochemistry, which is why there is a substantial body of literature on the study of the different processes (ion transfer, assisted ion transfer and electron transfer) that take place at the liquid/liquid (LL) interface. Electrochemistry at ITIES is rather complicated, and bipolar electrochemistry is a very useful tool to test electrochemical systems that, subsequently, can be studied by LL electrochemistry. Although new spectroelectrochemical setups have been successfully developed for LL interfaces,[20–29] the improvement of bipolar setups has been limited to electrochemical and electrochemiluminescence studies.[30–32] Bipolar electrochemistry has been used significantly less than electrochemistry at the ITIES, but the development of new devices should be decisive for a number of applications. For these reasons, the main objective of this technical note is the combination of bipolar electrochemistry with different spectroscopic techniques using a simple, versatile and functional spectroelectrochemical device. Spectroelectrochemistry is an effective way to obtain important information about the processes that occur at LL interfaces.[20–29] The selection of spectroscopic and electrochemical techniques among different spectral regions and multiple electrochemical procedures respectively, depends on the system studied.[33,34] UV-vis absorption spectroscopy is

perhaps the most used technique in spectroelectrochemistry and has been used for studying different types of chemical processes.[35–37] Developments in Raman spectroelectrochemistry have highlighted this technique as one of the best to characterize and study different materials and processes in many fields.[38–42] In the present work, most of the experiments were performed using UV-vis absorption spectroelectrochemistry, although Raman spectroelectrochemistry provided suitable information in the study of particular systems, as for example, carbon nanotubes.

One of the main highlights of the new bipolar device is its easy assembly. This simplicity allows us a fast and simple way for monitoring electron transfer reactions by UV-vis absorption spectroelectrochemistry or Raman spectroelectrochemistry. Another remarkable feature of this device is its versatility, since it allows the use of not only a wide variety of electrolytes and setup geometries, but also the study of systems with completely different electrochemical and/or optical properties. Three electrochemical systems were selected to illustrate the suitable performance of this new bipolar spectroelectrochemistry device: (1) reversible redox couples, such as different complexes of Ru (III/II), Fe (III/II) and Ir (IV/III), (2) the behavior of a film of single-walled carbon nanotubes (SWCNTs) during charge transfer processes between the two solutions, and (3) the electrosynthesis of a conducting polymer, poly(3,4-ethylenedioxythiophene) (PEDOT).

The first system studied, consisted of tris(2,2′-bipyridine)ruthenium (II) in one compartment and potassium hexacyanoferrate (III/II) in the other one. This ruthenium complex, $Ru(bpy)_3^{2+}$, has been previously studied in different spectroelectrochemical configurations and is commonly used as a model reaction at LL interfaces.[23,27,28,43] Meanwhile, the potassium hexacyanoferrate (III/II) redox couple is a one-electron, well-defined electrochemical system widely used as a probe in aqueous solution. The study of this system allowed us the spectroelectrochemical validation of the new device. The versatility of this device was demonstrated using different solvents. For that purpose, the second system analyzed consisted of 1,1'-dimethylferrocene (DMFc) in 1,2-dichlorobenzene (DCB) solution in one compartment, and potassium hexacyanoferrate (III/II) aqueous solution in the other one. Furthermore, two single-walled carbon nanotubes (SWCNT) films were used as bipolar electrode in order to study concomitantly the charge transfer reactions between the two solutions, and the behavior of the SWCNTs during the electron transfer process occurring through them. Finally, the last system analyzed in this work involved 3,4-ethylenedioxythiophene (EDOT) in one compartment and hexachloroiridate (IV/III) couple in the other one.

The main objective of this technical note is to demonstrate the correct performance of the new bipolar spectroelectrochemical cell, showing the capabilities and advantages of this novel device.

EXPERIMENTAL SECTION

Fabrication of the Bipolar Spectroelectrochemistry Device. A schematic representation of the newly-developed bipolar cell is shown in Figures 1 and S1. It consists of three parts: (1) support, (2) glassy carbon (GC) foil as bipolar electrode, allowing the electric connection bridging the two solutions and (3) the polytetrafluoroethylene (PTFE) built piece, which is fabricated using a CO_2 laser-cutting machine. PTFE has two compartments completely separated, and thereby, it avoids the mixture of the two solutions and the possibility of ion and assisted ion transfer reactions. These holes are 6 mm in depth, and 3.5 mm in diameter at the bottom and 6.5 mm at the top, with small volumes required. The bigger diameter allows the placement of reference (RE) and counter (CE) electrodes without interfering with either the optical fiber probe or the laser pathway. RE and CE are placed horizontally, through small holes at the side of the corresponding compartments. Two small recesses next to each compartment are useful to contain any solution leaked, avoiding the possible mixing of the two solutions. Furthermore, two O-rings, one for each compartment, are used to prevent electrolyte leakage and to facilitate the assembly of the cell.

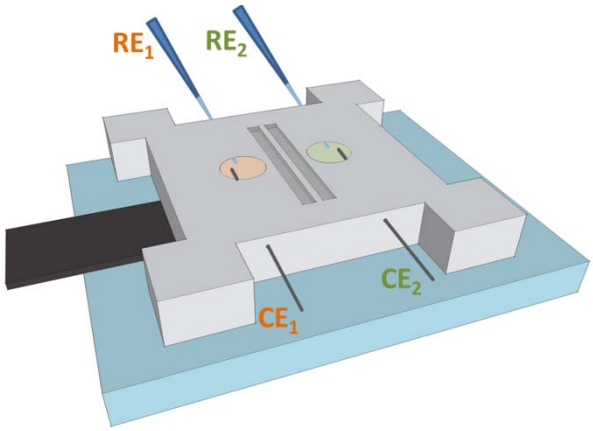

Figure 1. Bipolar spectroelectrochemistry cell. Schematic view of the disassembled cell is shown in Figure S1.

UV-vis measurements were performed introducing the optical reflection probe perpendicular to the GC foil in the compartment analyzed or two reflection probes concomitantly in the two phases. Raman measurements were carried out using an optical window placed on top of the PTFE piece to ensure a clear optical path for the laser, guarantee the flatness required to perform Raman spectroscopy measurements, and favor the collection of Raman photons. Hence, the cell design is optimal to place the UV-vis reflection probes in normal configuration in one or two compartments, to ensure the flatness of the solution required for Raman measurements, to facilitate the complete disassembly of the device to be cleaned, and to avoid any solution leakage.

RESULTS AND DISCUSSION

The bipolar spectroelectrochemical cell was used to study the electron transfer reaction that takes place at completely different systems, such as redox couples, carbon nanotubes films and electropolymerization processes.

$Ru(bpy)_3^{2+}$/$Fe(CN_6)^{4-}$, $Fe(CN_6)^{3-}$, system. In order to validate the bipolar spectroelectrochemical cell, reversible redox couples were chosen. The composition used in the spectroelectrochemical cell, Ag(s) | AgCl (s) | 0.5 mM $Ru(bpy)_3^{2+}$ + 0.5 M KCl (aq) || 25 mM $Fe(CN_6)^{4-}$ + 25 mM $Fe(CN_6)^{3-}$ + 0.5 M KNO_3 (aq) | AgCl(s) | Ag (s), prevents coupled reactions as oxygen or proton transfer processes. Electron transfer process was studied by cyclic voltammetry (CV), scanning the potential from -0.55 V to -0.90 V and back to -0.55 V at a scan rate

of 0.025 V s^{-1} (green line in Figure 2b). Initially, as the $Ru(bpy)_3^{2+}$ was just present in the reduced form, only the $Ru(bpy)_3^{2+}$ could be oxidized to $Ru(bpy)_3^{3+}$ during the forward scan while the reduction of $Fe(CN_6)^{3-}$ to $Fe(CN_6)^{4-}$ occurred in the other compartment. UV-vis absorption spectroelectrochemistry allowed us to study the redox reactions that took place in the two compartments simultaneously. In all experiments, the reference spectrum was taken before applying the potential to the cell. Figure 2a displays the UV-vis spectra in the Ru(II) solution. The integration time for UV-vis absorptiometric spectra was 100 ms, which indicates the high time-resolved data acquisition offered by this bipolar setup.

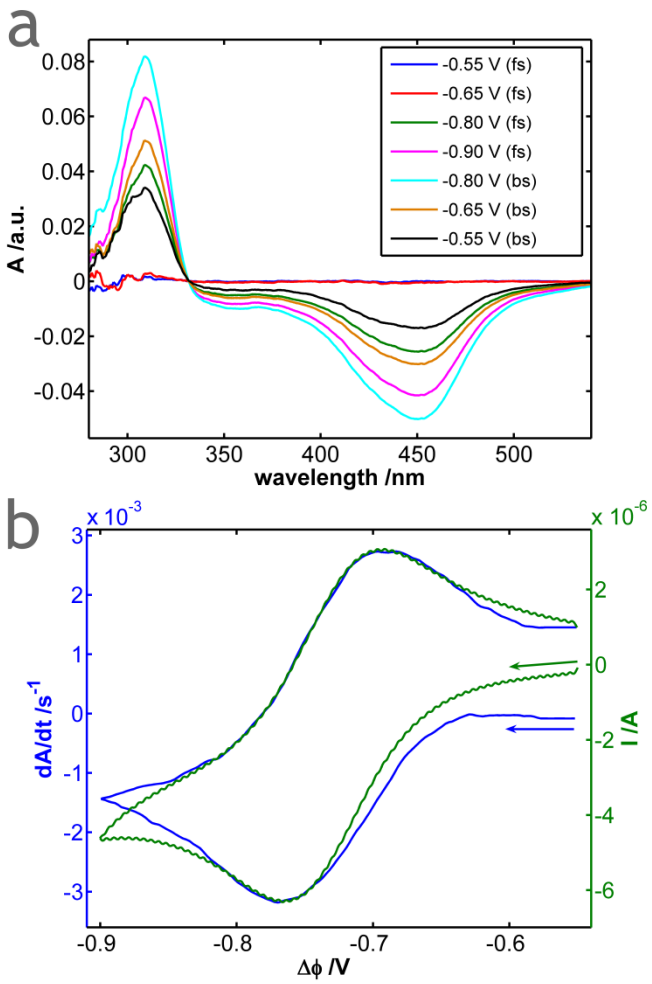

Figure 2. (a) UV-vis spectra evolution recorded in the $Ru(bpy)_3^{2+}/Ru(bpy)_3^{3+}$ compartment (integration time 100 ms) during the forward (fs) and backward (bs) scans. (b) Comparison between CV (green line) and derivative voltabsorptogram at 450 nm (blue line).

Three main bands are observed at 310, 385 and 450 nm, related to the redox reaction of $Ru(bpy)_3^{2+}$ (Figure 2a). Figure S2a illustrates the evolution of the band at 450 nm with potential. The absorbance at 450 nm decreases during the oxidation of $Ru(bpy)_3^{2+}$ to $Ru(bpy)_3^{3+}$, reaching the minimum value just before the reduction of the $Ru(bpy)_3^{3+}$ starts. Finally, the absorbance recovers similar values to the initial absorbance. Evolution of absorbance at 385 nm with potential shows the same behavior than the band at 450 nm, both bands relating to the consumption of $Ru(bpy)_3^{2+}$. However, the voltabsorptogram at 310 nm (Figure S2b) shows significant differences respect to 450and 385 nm bands. The absorbance at 310 nm increases during the forward scan and decreases during the backward one, indicating that is related to the electrogeneration of $Ru(bpy)_3^{3+}$.The high time-resolved data acquisition allows us to perform the derivative of absorbance with respect to time. The blue line in Figure 2b displays the derivative of absorbance at 450 nm and, as can be observed, it matches exactly the CV (green line, Figure 2b), showing one peak at -0.77 V during the forward scan and another at -0.70 V during the backward scan. The good agreement of the behavior of the derivative of absorbance with potential at 450 nm (blue line, Figure 2b) and the CV (green line, Figure 2b) demonstrates that the electrochemical peaks are only related to the redox couple $Ru(bpy)_3^{2+}/Ru(bpy)_3^{3+}$ and consequently, no secondary compounds are formed. In the case of the $Fe(CN_6)^{4-}/Fe(CN_6)^{3-}$ solution (Figure S3a), two bands are observed at 310 and 420 nm, related to the ferricyanide that is consumed during the redox process. Figure S3b shows the similarity between the derivative of absorbance at 420 nm (blue line) and the CV (green line), indicating that the spectroscopic response also reproduces the electrochemical behavior. Hence, the bipolar spectroelectrochemistry device has been validated using two reversible redox couples, providing very good results.

DMFc/$Fe(CN_6)^{4-}$, $Fe(CN_6)^{3-}$, system. A second system, formed by $Fe(CN_6)^{4-}/Fe(CN_6)^{3-}$ in aqueous solution in one compartment and DMFc in DCB in the other one, was studied to demonstrate the versatility of the new bipolar device using different solvents. The results displayed in Figure S4 show the high similarity between the CV and the spectroscopic changes related, in this case, to DMFc oxidation. Furthermore, the bipolar electrode was modified transferring a SWCNT film to each compartment of the GC foil. In this case, Raman spectroelectrochemistry was selected to monitor the behavior of the SWCNTs during the electrochemical process, where doping and de-doping of SWCNT films were observed simultaneously with the oxidation of DMFc (Figure S5). The results shown in Figures S4 and S5 demonstrate the good performance of the bipolar device for non-aqueous solvents and its versatility with respect to different spectroscopic techniques.

EDOT / $IrCl_6^{3-}$, $IrCl_6^{2-}$ system. In addition to reversible redox couples, systems of different nature were also studied. In the last example and, as proof of concept, the electropolymerization of EDOT was performed using the following composition of the bipolar cell: Ag(s) | AgCl (s) | 0.01 EDOT + 0.1 M LiCl (aq) || 1 mM $IrCl_6^{2-}$+ 0.1 mM $IrCl_6^{3-}$+ 0.1 M LiCl (aq) | AgCl(s) | Ag (s). EDOT electropolymerization was carried out by CV, scanning the potential from -0.90 V to +1.30V and back to -0.90 V five times at a scan rate of 0.250 V s^{-1} (Figure 3a). Figure 3b illustrates the UV-vis spectra recorded in the EDOT compartment. Different absorption bands are observed at 550, 650 and 750 nm, whose evolution with potential show different behavior during the EDOT electropolymerization. Absorbance at 550 and 650 nm increases slightly at potentials higher than +0.50 V, when the monomer and the electrogenerated polymer are oxidized (Figures S6a and S6b). However, the most significant change of the absorbance takes place at potentials lower than +0.50 V, during the backward scan, when the neutral polymer is formed; bands centered at 550 and

650 nm are related to neutral PEDOT. On the other hand, the absorbance at 750 nm increases from +0.30 V onwards during the forward scan, when doped PEDOT is formed, and decreases when the neutral PEDOT is electrogenerated during the backward scan (Figure S6c). UV-vis spectra of the $IrCl_6^{3-}$/$IrCl_6^{2-}$ compartment (Figure 3c), obtained simultaneously, show several bands centered at 265, 300, 430, 488 and 580 nm. All these bands display identical evolution with potential. Thus, the evolution of the band at 430 nm shown in Figure S7 can be considered as representative of the $IrCl_6^{2-}$ bands. Figure S7 shows that the absorbance does not change until a potential of 0.00 V is reached. At higher potentials, the intensity of this band decreases not only to the positive vertex but also until the potential returns to 0.00 V in the backward scan. Thereby, it is clear that the reduction of Ir(IV) to Ir(III) and the electropolymerization of EDOT at positive potentials are simultaneous processes.

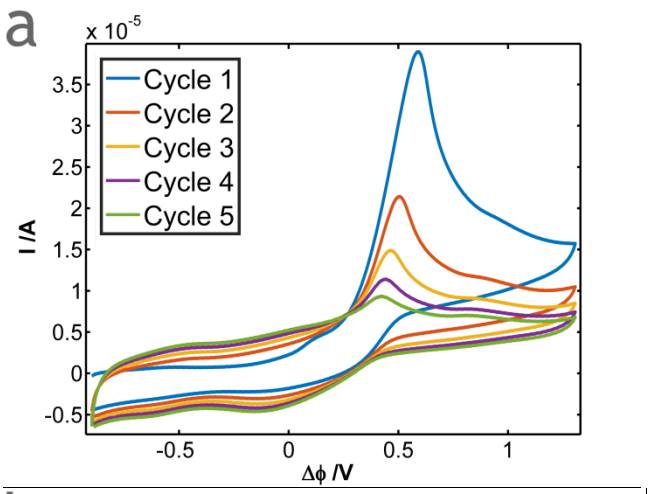

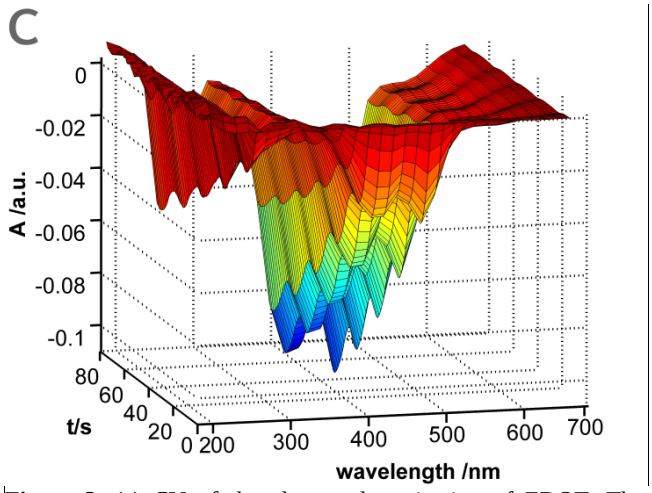

Figure 3. (a) CV of the electropolymerization of EDOT. The potential was scanned from -0.90 V to +1.30 V and back to -0.90 V five times at a scan rate of 0.250 V s^{-1}. UV-vis spectra recorded in (b) the EDOT compartment (integration time 25 ms) and in (c) the $IrCl_6^{3-}$/$IrCl_6^{2-}$ compartment (integration time 150 ms).

In order to control the electropolymerization of EDOT from the iridium compartment, the concentration of $IrCl_6^{2-}$ and $IrCl_6^{3-}$ were halved. Electrosynthesis of PEDOT was also performed by CV (5 cycles) at a scan rate of 0.250 V s^{-1}, although in this case a more positive potential was required (+1.50 V) to carry out the polymerization. UV-vis spectra of the EDOT compartment show the same PEDOT bands at 550, 650 and 750 nm than in the previous experiment using a higher concentration (Figure 3b). Figure 4 displays the comparison of the evolution of the band at 650 nm for the two different concentrations of the $IrCl_6^{3-}$/$IrCl_6^{2-}$ couple. As can be observed, the absorbance values are lower when the concentration of the $IrCl_6^{3-}$/$IrCl_6^{2-}$ couple decreases. The electropolymerization of EDOT can be controlled by changing the concentration of the redox couple presents in the other compartment. A lower amount of PEDOT was electrosynthesized when the concentration of the $IrCl_6^{3-}$/$IrCl_6^{2-}$ couple was decreased. These experiments demonstrate that using this new setup, the electropolymerization process can be controlled in two different ways: (1) by adjusting the potential during the scan, and (2) by limiting the current intensity with the concentration of the reversible couple. This two-way control of the polymerization process should be very useful to optimize the type of polymer generated on the electrode, taking advantage of both, potentiostaic and galvanostatic electropolymerization.

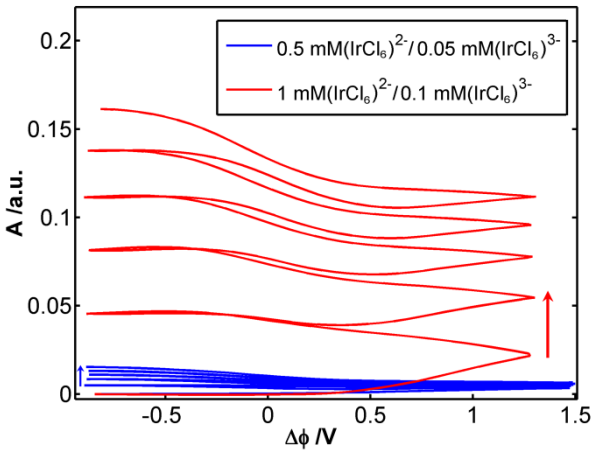

Figure 4. Comparison between the voltabsorptogram at 650 nm using different concentrations of the $IrCl_6^{3-}/IrCl_6^{2-}$ couple: 0.05 mM $IrCl_6^{3-}$/0.5 mM $IrCl_6^{2-}$ (blue line), and 0.1 mM $IrCl_6^{3-}$/1 mM $IrCl_6^{2-}$ (red line).

CONCLUSIONS

Recent works on bipolar electrochemistry, along with the development of new devices, make this technique one of the most attractive tools not only for analysis but also for material science. Although bipolar electrochemistry is not frequently used, the recent increase of interest during the last decade seems to bring back to life this powerful technique. The coupling of bipolar electrochemistry and spectroscopy provides the advantages of both techniques and furthermore, offers exceptional analytical possibilities. In this technical note, a novel and easy-to-use bipolar device has been fabricated, that has allowed us to study charge transfer processes that take places between two compartments completely separated. Traditionally, the study of the interface formed between two immiscible electrolyte solutions has been performed using devices in which the two compartments are in direct contact. However, these setups enable the coupling of ion, assisted ion and electron transfers, and also secondary complex reactions, making distinguishing the contribution of each reaction difficult. The new device presented in this work allows the elimination of ion and assisted ion transfer contributions and it ensures only electron transfer processes. Different systems were selected to illustrate the suitable performance of the new bipolar device, obtaining good and interesting results in all of them. The new bipolar device allows us, in a fast and simple way, to monitor the electron transfer at different compartments using spectroelectrochemistry. According to the results presented in this work, this novel bipolar spectroelectrochemistry device shows a number of highly interesting issues that invite further studies of charge transfer reactions in a wide range of analytical applications.

ASSOCIATED CONTENT

Supporting Information

The Supporting Information is available free of charge on the ACS Publications website.

Experimental section; schematic view of the disassembled bipolar cell; cyclic voltammograms; UV-vis spectra; UV-vis voltabsorptograms; and evolution of Raman G-band of SWCNT with potential (PDF).

AUTHOR INFORMATION

Corresponding Authors

*E-mail: dibanez@ubu.es
*E-mail: acolina@ubu.es
Tel: +34 947 25 88 17. Fax: +34 947 25 88 31.

Author Contributions

The manuscript was written through contributions of all authors. All authors have given approval to the final version of the manuscript.

Notes

The authors declare no competing financial interest.

ACKNOWLEDGMENT

Financial support from Ministerio de Economía y Competitividad (CTQ2014-55583-R, CTQ2014-61914-EXP, CTQ2015-71955-REDT) and Junta de Castilla y León (BU033-U16) is gratefully acknowledged. D.I. thanks Ministerio de Economía y Competitividad for his post-doctoral fellowship (CTQ2014-61914-EXP). Dr. Daniela Plana is acknowledged for her help in the development of this technical note.

REFERENCES

(1) Kazdobin, K.; Shvab, N.; Tsapakh, S. *Chem. Eng. J.* **2000**, *79*, 203–209.
(2) Livshits, V.; Blum, A.; Strauss, E.; Ardel, G.; Golodnitsky, D.; Peled, E. *J. Power Sources* **2001**, *97-98*, 782–785.
(3) Pretorius, W. A.; Johannes, W. G.; Lempert, G. G. *Water SA* **1991**, *17*, 133–138.
(4) Fleischmann, M.; Ghoroghchian, J.; Rolison, D.; Pons, S. *J. Phys. Chem.* **1986**, *90*, 6392–6400.
(5) Loget, G.; Kuhn, A. *J. Mater. Chem.* **2012**, *22*, 15457–15474.
(6) Loget, G.; Roche, J.; Gianessi, E.; Bouffier, L.; Kuhn, A. *J. Am. Chem. Soc.* **2012**, *134*, 20033–20036.
(7) Loget, G.; Zigah, D.; Bouffier, L.; Sojic, N.; Kuhn, A. *Acc. Chem. Res.* **2013**, *46*, 2513–2523.
(8) Chow, K.-F.; Chang, B.-Y.; Zaccheo, B. A.; Mavré, F.; Crooks, R. M. *J. Am. Chem. Soc.* **2010**, *132*, 9228–9229.
(9) Laws, D. R.; Hlushkou, D.; Perdue, R. K.; Tallarek, U.; Crooks, R. M. *Anal. Chem.* **2009**, *81*, 8923–8929.
(10) Loget, G.; Kuhn, A. *Anal. Bioanal. Chem.* **2011**, *400*, 1691–1704.
(11) Chow, K.-F.; Mavré, F.; Crooks, R. M. *J. Am. Chem. Soc.* **2008**, *130*, 7544–7545.
(12) Chang, B.-Y.; Chow, K.-F.; Crooks, J. A.; Mavré, F.; Crooks, R. M. *Analyst* **2012**, *137*, 2827–2833.
(13) Zhang, X.; Chen, C.; Yin, J.; Han, Y.; Li, J.; Wang, E. *Anal. Chem.* **2015**, *87*, 4612–4616.
(14) Mavré, F.; Anand, R. K.; Laws, D. R.; Chow, K.-F.; Chang, B.-Y.; Crooks, J. A.; Crooks, R. M. *Anal. Chem.* **2010**, *82*, 8766–8774.
(15) Sentic, M.; Arbault, S.; Goudeau, B.; Manojlovic, D.; Kuhn, A.; Bouffier, L.; Sojic, N. *Chem. Commun.* **2014**, *50*, 10202–10205.
(16) Bouffier, L.; Arbault, S.; Kuhn, A.; Sojic, N. *Anal. Bioanal. Chem.* **2016**, *408*, 7003–7011.
(17) Bouffier, L.; Doneux, T.; Goudeau, B.; Kuhn, A. *Anal. Chem.* **2014**, *86*, 3708–3711.
(18) Chang, B.-Y.; Mavré, F.; Chow, K.-F.; Crooks, J. A.; Crooks, R. M. *Anal. Chem.* **2010**, *82*, 5317–5322.
(19) Sequeira, C. A. C.; Cardoso, D. S. P.; Gameiro, M. L. F. *Chem. Eng. Commun.* **2016**, *203*, 1001–1008.
(20) Ding, Z.; Fermín, D. J.; Brevet, P.-F.; Girault, H. H. *J. Electroanal. Chem.* **1998**, *458*, 139–148.
(21) Duong, H. D.; Brevet, P. F.; Girault, H. H. *J. Photochem. Photobiol. A Chem.* **1998**, *117*, 27–33.
(22) Fermín, D. J.; Ding, Z.; Brevet, P.-F.; Girault, H. H. *J. Electroanal.*

Chem. **1998**, *447*, 125–133.
(23) Ding, Z.; Wellington, R. G.; Brevet, P.-F.; Girault, H. H. *J. Electroanal. Chem.* **1997**, *420*, 35–41.
(24) Ishizaka, S.; Kim, H.-B.; Kitamura, N. *Anal. Chem.* **2001**, *73*, 2421–2428.
(25) Sperline, R. P.; Freiser, H. *Langmuir* **1990**, *6*, 344–347.
(26) Yordanov, S.; Best, A.; Butt, H.-J.; Koynov, K. *Opt. Express* **2009**, *17*, 21149–21158.
(27) Izquierdo, D.; Martinez, A.; Heras, A.; Lopez-Palacios, J.; Ruiz, V.; Dryfe, R. A. W.; Colina, A. *Anal. Chem.* **2012**, *84*, 5723–5730.
(28) Martínez, A.; Colina, A.; Dryfe, R. A. W.; Ruiz, V. *Electrochim. Acta* **2009**, *54*, 5071–5076.
(29) Ibañez, D.; Plana, D.; Heras, A.; Fermín, D. J.; Colina, A. *Electrochem. Commun.* **2015**, *54*, 14–17.
(30) Hotta, H.; Akagi, N.; Sugihara, T.; Ichikawa, S.; Osakai, T. *Electrochem. Commun.* **2002**, *4*, 472–477.
(31) Plana, D.; Jones, F. G. E.; Dryfe, R. A. W. *J. Electroanal. Chem.* **2010**, *646*, 107–113.
(32) Gründer, Y.; Fabian, M. D.; Booth, S. G.; Plana, D.; Fermín, D. J.; Hill, P. I.; Dryfe, R. A. W. *Electrochim. Acta* **2013**, *110*, 809–815.
(33) Dunsch, L. *J. Solid State Electrochem.* **2011**, *15*, 1631–1646.
(34) Keyes, T. E.; Forster, R. J. In *Handbook of Electrochemistry*; Zoski, C. G., Ed.; Elsevier: Amsterdam, 2007; pp 591–635.
(35) Ventosa, E.; Colina, A.; Heras, A.; Martínez, A.; Orcajo, O.; Ruiz, V.; López-Palacios, J. *Electrochim. Acta* **2008**, *53*, 4219–4227.
(36) Fernandez-Blanco, C.; Colina, A.; Heras, A.; Ruiz, V.; Lopez-Palacios, J. *Electrochem. Commun.* **2012**, *18*, 8–11.
(37) Weber, C. M.; Eisele, D. M.; Rabe, J. P.; Liang, Y.; Feng, X.; Zhi, L.; Müllen, K.; Lyon, J. L.; Williams, R.; VandenBout, D. A.; Stevenson, K. J. *Small* **2010**, *6*, 184–189.
(38) Ibañez, D.; Fernandez-Blanco, C.; Heras, A.; Colina, A. *J. Phys. Chem. C* **2014**, *118*, 23426–23433.
(39) Gómez, R.; Pérez, J. M.; Solla-Gullón, J.; Montiel, V.; Aldaz, A. *J. Phys. Chem. B* **2004**, *108*, 9943–9949.
(40) Ren, B.; Li, X. Q.; She, C. X.; Wu, D. Y.; Tian, Z. Q. *Electrochim. Acta* **2000**, *46*, 193–205.
(41) Kavan, L.; Dunsch, L. *ChemPhysChem* **2011**, *12*, 47–55.
(42) Ibañez, D.; Santidrian, A.; Heras, A.; Kalbáč, M.; Colina, A. *J. Phys. Chem. C* **2015**, *119*, 8191–8198.
(43) Ding, Z.; Wellington, R. G.; Brevet, P. F.; Girault, H. H. *J. Phys. Chem.* **1996**, *100*, 10658–10663.

Insert Table of Contents artwork here